Materials Science and Engineering C 42 (2014) 553–561

Contents lists available at ScienceDirect

Materials Science and Engineering C

journal homepage: www.elsevier.com/locate/msec

Chitosan–silica hybrid porous membranes

Christos Pandis [a,b,*], Sara Madeira [c], Joana Matos [c], Apostolos Kyritsis [a], João F. Mano [c,d], José Luis Gómez Ribelles [b,e]

[a] Physics Department, National Technical University of Athens, Zografou Campus, 15780 Athens, Greece
[b] Centro de Biomateriales e Ingeniería Tisular, Universitat Politècnica de València, Camino de Vera s/n, 46022 Valencia, Spain
[c] 3B's Research Group—Biomaterials, Biodegradables and Biomimetics, University of Minho, Headquarters of the European Institute of Excellence on Tissue Engineering and Regenerative Medicine, AvePark, 4806-909, Taipas, Guimarães, Portugal
[d] ICVS/3B's, PT Government Associate Laboratory, Braga, Guimarães, Portugal
[e] Ciber en Bioingeniería, Biomateriales y Nanomedicina (CIBER-BBN), Spain

ARTICLE INFO

Article history:
Received 19 February 2014
Received in revised form 3 May 2014
Accepted 30 May 2014
Available online 7 June 2014

Keywords:
Chitosan
Silica
Genipin
Scaffolds
Hybrid
Mechanical properties

ABSTRACT

Chitosan–silica porous hybrids were prepared by a novel strategy in order to improve the mechanical properties of chitosan (CHT) in the hydrogel state. The inorganic silica phase was introduced by sol–gel reactions in acidic medium inside the pores of already prepared porous scaffolds. In order to make the scaffolds insoluble in acidic media chitosan was cross-linked by genipin (GEN) with an optimum GEN concentration of 3.2 wt.%. Sol–gel reactions took place with Tetraethylorthosilicate (TEOS) and 3-glycidoxypropyltrimethoxysilane (GPTMS) acting as silica precursors. GPTMS served also as a coupling agent between the free amino groups of chitosan and the silica network. The morphology study of the composite revealed that the silica phase appears as a layer covering the chitosan membrane pore walls. The mechanical properties of the hybrids were characterized by means of compressive stress–strain measurements. By immersion in water the hybrids exhibit an increase in elastic modulus up to two orders of magnitude.

1. Introduction

Chitosan (CHT) is a linear polysaccharide derived from chitin, a naturally abundant organic material obtained mainly from the exoskeleton of the crustacean, for example lobsters, shrimps and insects as well as from the cell walls of some bacteria and fungi [1,2]. The deacetylation of chitin yields a copolymer composed of glucosamine and N-acetylglucosamine units linked by (1–4) glycosidic bonds. The degree of deacetylation (DD), defined as the ratio of glucosamine to the sum of glucosamine and N-acetylglucosamine, has influence in molecular weight, crystallinity, solubility, mechanical strength and biological properties of CHT and CHT-based biomaterials [3]. CHT does not dissolve in either organic solvents or in water at neutral or basic conditions but dissolves in acidic medium (pH < 6), for example in acetic and formic acids, due to protonation of free amino groups.

The biocompatibility, biodegrability [4], anti-bacterial activity, non-toxicity [4] and cellular compatibility of chitosan have boost the scientific research interest in the latest two decades to explore its use in biomedical applications [3]. Furthermore, its ability to be shaped in various forms such as films, microparticles [5], fibers [6] and porous scaffolds [7], its naturally hydrophilic character [8], the pH-dependent cationic nature and its tendency to interact with anionic glycosaminoglycans (GAGs), heparin, proteoglycans, and nucleotides like DNA or siRNA make CHT particularly suitable as a biomaterial for tissue repair and regeneration [9–11]. Due to its biological properties CHT is considered one of the most valuable polymer for biomedical and pharmaceutical applications such as drug delivery systems [5], surgical suture, dental implants, artificial skin, rebuilding of bone and cartilage, corneal contact lenses and encapsulating material, wound healing accelerator [12], weight loss effect, blood cholesterol control, artificial blood vessels and gene therapy. CHT has been shown to be osteoconductive in vitro and in vivo [13]. However, the mechanical properties of CHT are not adequate for bone regeneration because CHT has low Young's modulus especially in wet porous scaffolds.

The chemical modification of CHT appears as a promising method for the preparation of new materials based on chitosan with advanced physicochemical properties [14]. Furthermore, covalent and ionic cross-linking of chitosan is a very efficient approach to improve the properties of chitosan gels [15]. Tripolyphosphate (TPP) [16] is widely

* Corresponding author at: Physics Department, National Technical University of Athens, Zografou Campus, 15780 Athens, Greece.
E-mail address: pandis@mail.ntua.gr (C. Pandis).

http://dx.doi.org/10.1016/j.msec.2014.05.073
0928-4931/

used for physical cross-linking while the most common chemical cross-linkers used are dialdehydes such as glyoxal and in particular glutaraldehyde (GTA) [15]. However, in the field of biomedical technology genipin (GEN) [17,18], a cross-linker of natural origin, is often favored over GTA for chitosan cross-linking due to its advantages in terms of cytotoxicity [19].

Another very interesting approach for the preparation of new materials is the combination of chitosan with a second component to fabricate polymer blends and composites. Polymers, like gelatin [20], poly(vinyl alcohol) [21], poly(lactic acid) [22] and poly(ε-caprolactone) [23,24], to name a few, have been utilized for preparing blends with chitosan while inorganic materials, for example hydroxyapatite (HAp) [25], layered silicates [26], carbon nanotubes (CNTs) [27] and glass/ceramic particles [28–31], have been used to form chitosan composites. Especially for applications that mechanical reinforcement is required the incorporation of an inorganic phase into the chitosan matrix to form hybrid materials appears as a very effective strategy. Chitosan/silica hybrids have been prepared by mixing chitosan in the silane solution [32]. Reactions with 3-glycidoxypropyltrimethoxysilane (GPTMS) can link polymer chains to silica network through covalent bonds [33–35]. Furthermore, porous structures of chitosan/TEOS have been fabricated as described in references [36,37].

In this work silica was added in a previously formed chitosan scaffold in the form of a coating layer of the pore walls within the porous structure. The initial highly porous scaffolds were prepared by the freeze gelation technique [38]. CHT was cross-linked by GEN following the optimal procedure combined with the optimal mixture composition. The hybrids were produced by the in-situ synthesis of the silica inorganic part inside the pores of the scaffolds by sol–gel reactions [39] in acidic medium. Extending the successful procedure reported in previous publications of our group [40,41], in this work the coupling agent GPTMS was used in order to facilitate the wetting of the pores and to introduce chemical bonding between the organic and inorganic phases of the hybrid. The influence of silica incorporation in morphology, thermal and mechanical properties of chitosan scaffolds is assessed and discussed.

2. Experimental

2.1. Materials

Chitosan (CHT) with low molecular weight and deacetylation degree (DD) of 75–85% was purchased from Sigma–Aldrich. Acetic acid, hydrochloric acid and sodium hydroxide (NaOH) were supplied from Panreac. Genipin (GEN) was purchased from Wako Chemicals. 3-glycidoxypropyltrimethoxysilane (GPTMS) and tetraethyl orthosilicate (TEOS) were obtained from Sigma–Aldrich. Ultrapure (MilliQ) water was used in all preparation procedures.

2.2. Preparation of hybrids

2.2.1. Preparation of cross-linked films and scaffolds

A starting CHT solution obtained by dissolving 1.5 wt.% of CHT in 1% wt acetic acid was used in all the procedures for preparing films and scaffolds. The solution was left stirring for 24 h and then filtered using a 70 μm millipore membrane.

In order to study the effect of cross-linking and to decide on the optimal GEN concentration to be used later, chitosan films with varying cross-linking degree were prepared. To that end the appropriate amount of GEN was mixed with 30 mL of the above CHT solution to obtain 0.66, 3.2, 6.2, 14.2 and 25 wt.% of GEN in the final CHT films. The mixtures were placed into Petri dishes to react for 24 h at room temperature and the films were obtained by solvent casting. The films were washed repeatedly with distilled water in order to remove residues of GEN and immersed in a 0.5 M solution of NaOH to neutralize them. Finally, were dried at 40 ºC in vacuum for 24 h.

Highly porous scaffolds were prepared using the freeze-gelation method [38,42]. According to this method the chitosan solution being transferred in Teflon crystallizers was frozen at −80 °C using liquid nitrogen. Then the frozen chitosan was fully immersed in the gelification environment of NaOH 0.5 M in ethanol aqueous solution, precooled at −20 °C. The frozen chitosan was left immersed for 72 h at −20 °C, a temperature lower than its freezing point. In that way chitosan was gelled and the acetic acid solution was removed leaving a porous structure. Finally, the obtained scaffolds were cut into disks of 8 mm diameter and washed thoroughly with distilled water up to neutral pH.

The final cross-linked CHT scaffolds were prepared by the two methods, namely method I (metI) and method II (metII) presented schematically in Fig. 1 and described as follows:

2.3. Method I

The CHT solution was mixed directly with GEN under vigorous stirring for 1 h to make a mixture containing 3.2% of GEN referring to the final CHT cross-linked samples. The blend was placed into Teflon crystallizer to react for 24 h at room temperature. Scaffolds were obtained by the freeze-gelation method and finally lyophilized using a Telstar Lyoquest apparatus in order to be left dried and with the pores fully opened for the subsequent steps.

2.4. Method II

The already prepared scaffolds or films of pure CHT were immersed into aqueous GEN solution (0.0065% w/v) at room temperature for 48 h and protected from light. To remove the excess of GEN the cross-linked films and scaffolds were washed with distilled water repeatedly. Then, the scaffolds were freeze-dried at −80 ºC for 24 h and the films were dried under vacuum.

2.4.1. Introduction of silica by sol–gel

In a second step the silica precursors were introduced inside the pores of the lyophilized scaffolds. For this purpose, the silica network was synthesized in situ by the sol–gel method [39] using TEOS and GPTMS as precursors. The molar ratio of TEOS with respect to GPTMS in the sol–gel solution was either 1:0.1, 1:0.5 or 1:1 and the molar ratios of the rest of the components (water, ethanol and chloride acid) of the starting solution were kept constant (1, 2 and 0.0185, respectively) with respect to TEOS. After 1 h of stirring, the above solution was transferred to a glass tube fully covering the CHT scaffolds. In order to assure that the pores of the polymer will be filled by the precursor solution, a vacuum pump attached to the reaction tube was pumping for 5 min prior to the introduction of the solution. After being immersed for 15 min in the sol–gel solution the samples were superficially rinsed with water/ethanol. Then, the scaffolds with silica layers on the pore walls, were left at room temperature for 24 h and subsequently dried for 24 h. Finally, the samples were washed with distilled water for 4 h and then dried again at 50 °C in vacuum for 24 h. The weight content of the silica phase (including organic side chains of GPTMS) was calculated by the increase of weight of the membrane after sol–gel reaction (Table 3) ranging between 74 and 89 wt.% of the obtained hybrid. The content of SiO_2 can be estimated from the residual weight after pyrolysis which ranges between 26 and 43 wt.% (Table 3).

2.5. Material characterization

2.5.1. Morphology

The morphology of the CHT, CHT–GEN and CHT–GEN/silica scaffolds was studied by means of Scanning Electron Microscopy (SEM) using a JSM-6300 (JEOL) microscope, with the samples previously sputter coated with gold. Porosity was measured by a gravimetric method. The samples were weighed dried and then immersed into octane in

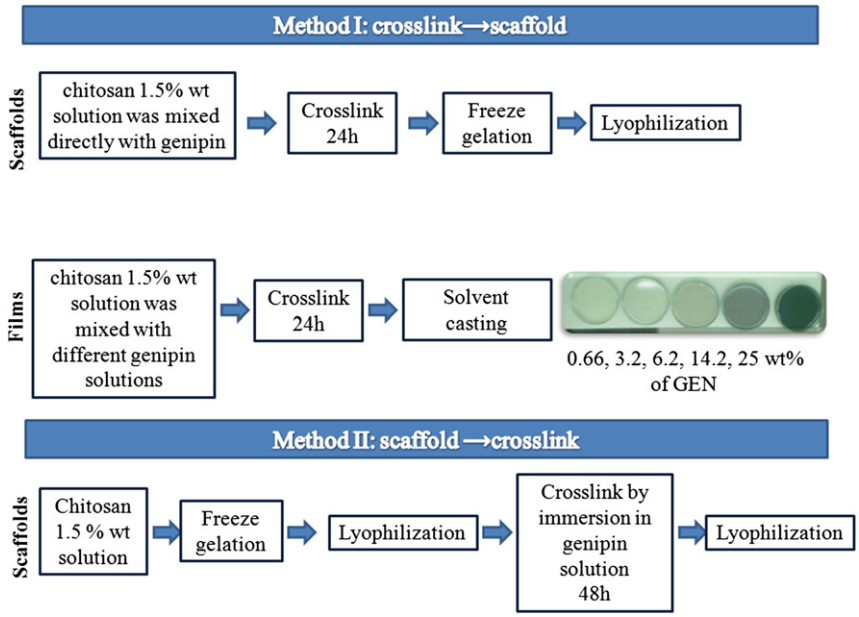

Fig. 1. Methods used for the preparation of genipin cross-linked chitosan films and scaffolds.

order to have the pores filled. Porosity, p (%), was calculated as the quotient of the volume of pores (V_{pore}) and the total volume of the scaffold (V_{sc})

$$p(\%) = \frac{V_{pore}}{V_{sc}} * 100 = \frac{V_{pore}}{V_{polym} + V_{pore}} * 100. \quad (1)$$

The volume occupied by the pores, V_{pore}, was deduced from the weight difference between dry (m_{dry}) and wet (m_{wet}) sample,

$$V_{pore} = \frac{m_{wet} - m_{dry}}{\rho_{octane}} \quad (2)$$

where the density of octane (ρ_{octane}) is 0.79 g/cm^3. The chitosan volume, V_{polym} was calculated by $V_{polym} = m_{CHT}/\rho_{CHT,}$ where density of CHT (ρ_{CHT}) was taken as 1.25 g/cm3.

The water absorption capacity of scaffolds and films was determined by immersing them in phosphate buffered saline (PBS) solution (pH = 7.4) at room temperature for 1, 3 and 24 h. The amount of absorbed water was calculated as

$$W(\%) = \left(\frac{m_{wet} - m_{dry}}{m_{dry}}\right) * 100 \quad (3)$$

where w_{dry} is the mass of dry scaffold and m_{wet} is the weight of scaffold after being immersed in PBS.

2.5.2. Solubility in acidic medium-extent of cross-linking

To study the solubility of CHT in acidic medium, the samples were immersed in a 1% acetic acid solution. The degree of cross-linking was quantified by performing the ninhydrin assay [43]. This test was used as the indicator of the free amino groups existing in both, the pure and cross-linked chitosan samples. The blue reaction product of ninhydrin with free amino groups has a maximum absorbance at 567 nm in isopropanol. The optical absorbance of the solution was recorded with a UV–visible spectrophotometer (CECIL 9000) at 567 nm. Glycine at various known concentrations was used as reference in order to construct the standard curve.

2.5.3. Hybrid composition–thermal properties

Pyrolysis residue was determined by heating the samples at 850 ºC for at least 2 h in air atmosphere using an electrical tubular oven (Gallur).

The thermal properties of samples were studied by thermogravimetric analysis (TGA) using a SDT-Q600 (TA-Instruments) equipment in nitrogen atmosphere with a constant heating rate of 10 ºC/min from 30 ºC to 800 °C. Differential scanning calorimetry (DSC) measurements were performed in a DSC 8000 (Perkin Elmer) from −80 ºC to 150 ºC with a heating and cooling rate of 10 ºC/min using nitrogen as purge gas.

2.5.4. Mechanical property characterization

Dynamic mechanical analysis (DMA) measurements were carried out on dried and wet CHT and CHT–GEN films using a DMA 8000 (Perkin Elmer) apparatus. Thermo-mechanical analysis (TMA) measurements were carried out on CHT, CHT–GEN and CHT–GEN reinforced with silica. The stress–strain curves were recorded upon compression by means of a TMA/SS6000 (SII Seiko Instruments) on samples immersed in water.

3. Results and discussion

3.1. Chitosan cross-linked by genipin

3.1.1. Solubility in acidic medium

The primary goal of the essay regarding cross-linking of chitosan was to find the lower genipin concentration that renders chitosan scaffolds insoluble in acidic medium. To that aim cross-linked chitosan films and scaffolds with various GEN concentrations with respect to final CHT samples were prepared by the two methods presented in Fig. 1. The mixing time of CHT solution with genipin before casting to Teflon molds was limited to 30 min. For mixing times longer than 60 min the gels become very viscous and are not transferable from the mixing vial. The above observation is confirmed by dynamic oscillatory rheology studies in genipin cross-linked biopolymers containing primary amide groups [44]. It is well known that the short chains of genipin act as cross-linking bridges between amino groups of chitosan [17]. By increasing GEN concentration the resulting color of the films varied from light to dark blue-green as can be seen in Fig. 1. The characteristic dark-blue coloration that appears in the genipin cross-linked hydrogels

exposed to air is associated with the oxygen radical-induced polymerization of genipin as well as its reaction with amino groups. It is worth noting that for the method II a reaction time of 24 h was not enough to complete the cross-linking and only after 48 h the films had the characteristic of bluish color indicating completion of cross-linking which makes chitosan gels insoluble in acidic medium.

Solubility tests were performed by immersing the films and scaffolds prepared by method I in 1% acetic acid solution. Pure chitosan films and scaffolds were dissolved after a few minutes, as expected, and the same was observed for the samples with 0.66 wt.% of GEN. The rest of the samples with higher concentration of GEN remained insoluble in the test solution even for weeks after the immersion. The above result was the decisive fact for choosing the GEN concentration to be 3.2 wt.% for preparing cross-linked films and scaffolds. As already stated chitosan is cross-linked by genipin through amino groups of chitosan. For the purpose of obtaining a hybrid material with links between the organic and inorganic phase it was desirable that a great amount of amino groups being left unreacted after cross-linking in order to react with GPTMS in the subsequent step of the preparation procedure.

The effect of CHT cross-linking with GEN was quantified by the ninhydrin assay. Table 1 depicts the number of moles of amino groups per mg of sample of pure CHT and CHT–GEN prepared by the two methods. The above results clearly show the reduction of the number of moles of free amino groups of CHT after cross-linking. Furthermore, higher cross-linking degree is observed for the samples prepared by method I. The direct mixing of genipin with the chitosan solution allows a reaction of higher yield compared to cross-linking of already formed chitosan film by the immersion into a genipin solution. Thus, the first method appears favorable as it is more straightforward and with higher yield. Furthermore, it is simpler and less energy and time consuming as it comprises only one step of lyophilization.

3.1.2. Effect of genipin cross-linking

Fig. 2 shows representative micrographs obtained from the SEM study. The pure uncross-linked chitosan depicted in Fig. 2 presents the typical structure of chitosan scaffolds prepared by the freeze-gelation technique [45]. It is well known that the final structure is influenced by the molecular weight of CHT [46], the concentration of CHT [47] in the starting solution as well as by the freezing process [42]. In our case the use of 1.5 wt% CHT in the starting solution and the rapid cooling using liquid nitrogen leads to scaffolds with thin walls, interconnected pores with length of tens of microns and porosity of 95% as evaluated by gravimetric techniques and listed in Table 3. The above topology characterized with high pore surface is adequate for possible cell attachment and differentiation [48]. No noticeable differences regarding porous morphology are observed when comparing pure CHT scaffolds and CHT–GEN metI (Fig. 2) or CHT–GEN metII (not shown here).

The influence of genipin concentration and consequently the degree of cross-linking on the mechanical properties was studied on both, dry and water swollen films. The results obtained from stress–strain tests under tensile loading are reported in Table 2 for samples with varying genipin content. The elastic modulus of swollen pure CHT and CHT–GEN with 0.66 wt.% GEN was too low, out of the measuring window of the instrument. The increase of E' value from 1950 MPa for neutralized CHT sample to 2320, 3580 and 3750 MPa respectively for 0.66, 3.2 and 6.2 wt.% of GEN is a consequence of the material stiffening by cross-linking. Furthermore, the hydrogel character of chitosan is evident as well as the softening effect of water which upon immersion leads to a decrease of the elastic modulus by more than three orders of magnitude.

Fig. 3a depicts the swelling behavior of the films cross-linked with method I after being immersed in water for 1 h, 3 h and 24 h. The swelling degree of the pure CHT film is calculated to be close to 400%. The swelling ability decreases almost to the half for the GEN cross-linked films. By further increasing the amount of the cross-linker no significant changes are observed within the error of the measurement. Furthermore, it could be seen that the films have reached the highest capacity of water absorption already from the first hour of immersion. Fig. 3b presents water uptake of pure CHT and CHT–GEN porous scaffolds cross-linked by both methods. In those swollen samples water is fully filling the pores, thus water uptake depends mainly on porosity and cross-linking plays a minor role in water sorption. The results shown in Fig. 3 support the SEM observations and the porosity results in the sense that microstructure of the scaffolds is not significantly affected by cross-linking.

From this point forward all the genipin cross-linked chitosan scaffolds used for the incorporation of silica prepared by the two methods (method I or method II) are assigned as CHT_{genI} and CHT_{genII} respectively.

Table 1
Number of free amino groups of CHT scaffolds cross-linked with GEN by methods I and II.

Sample	Number of moles NH_2/mg
CHT pure	3.52E-06
CHT–GEN met I	1.75E-06
CHT–GEN met II	2.78E-06

3.2. Chitosan/Silica hybrids by sol–gel

3.2.1. Morphology

The high porosity and the interconnectivity of the pores allow the efficient introduction of the silica precursor solution inside the scaffolds. The penetration of the solution in the interior of the scaffolds is further facilitated by the use of a vacuum pump during the preparation procedure. The concentration of the solution, the water/TEOS ratio and mainly the pH determines the final morphology of the in situ produced silica. It is well established that basic conditions lead to the production of silica in the form of branched species and microparticles [39,41] while acidic conditions result in a continuous silica phase. In this work we have used acidic conditions in order to promote the formation of a silica layer covering the CHT walls of the pores. Previous works have shown that the final morphology of silica phase is affected by the properties of the polymer matrix. In PCL porous membranes, which is a highly hydrophobic polymer, we have seen that silica coating on pore walls is formed when sol–gel is performed in acidic conditions [41,49]. On the contrary, in the case of a microporous PHEA hydrogel the solution not only fills the pores but it is absorbed by the pore walls as well [19]. The result after sol–gel reaction is a non-porous composite with a silica phase consisting in interconnected nano and micro-domains [19] because silica is formed into the nanopores of the hydrogel as well as in the macropores of the membrane, and silica interconnectivity collapses any remaining empty spaces. In the present case the starting solution easily penetrates the porous structure but does not swell significantly the CHT scaffolds. Thus, after the completion of the sol–gel reactions a porous hybrid scaffold is obtained. In Table 1 the coding of the hybrids that will be followed throughout the paper is reported. The increase of the residue weight, as evaluated by pyrolysis and TGA measurements (Table 1, results that will be further discussed later) indicates the presence of the silica phase. Furthermore, the results concerning the porosity of the resulting hybrid scaffolds as determined by gravimetric techniques are listed in the same table. The porosity decreases with respect to the original membrane, as expected. Volume fraction of pores depends on the amount of GPTMS used in the starting solution, a fact permitting its modulation. Furthermore, GPTMS serving as a coupling agent promotes the wetting of the CHT walls and hypothetically the chemical bonding with them.

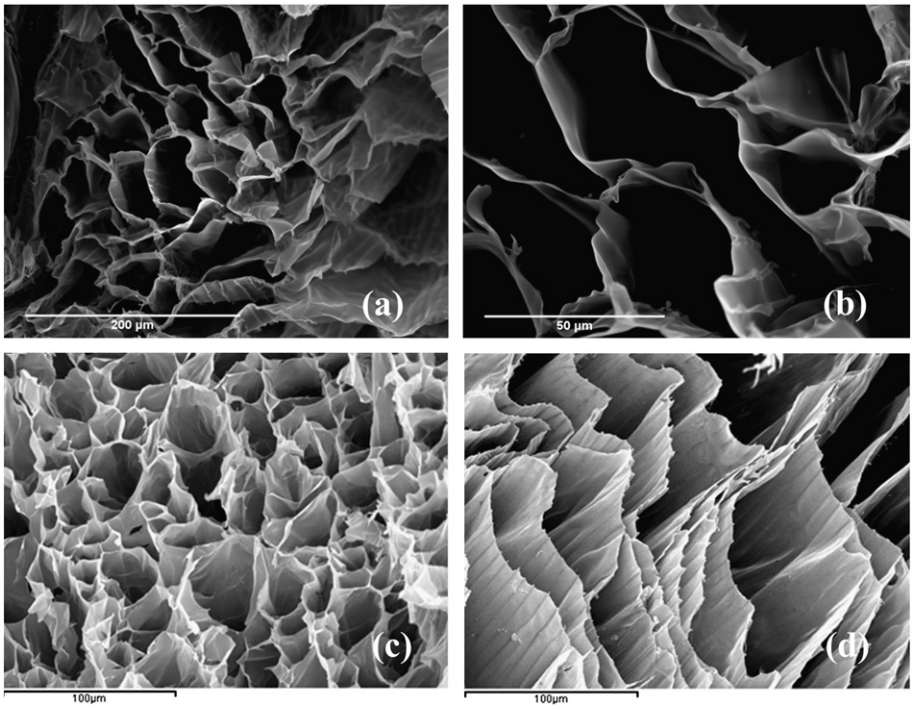

Fig. 2. Morphology of pure CHT (a,b) and CHT–GEN (c,d) scaffolds.

Indeed, Connell et al. [50] in a thorough study using solution and solid state Nuclear Magnetic Resonance (NMR) techniques have confirmed that the epoxide group of GPTMS can react with the primary amine of chitosan allowing covalent coupling of the polymer with the silica network. Furthermore, they have shown that the acidic conditions favor also the side reaction of water with the epoxide group of GPTMS to form diol at a ratio of 80% irrespectively of pH. As both reactions are acid catalyzed [51] the use of a very low pH ~ 1 in the present study is expected to result in the covalent bonding of GPTMS with chitosan as well as in the formation of diols from GPTMS.

SEM analysis allowed the assessment of the hybrid scaffold morphology showing that the porous structure of the scaffolds is retained as evidenced in Fig. 4a. A careful observation of the Fig. 4b reveals that the added inorganic phase partially fills the pores and, thus, contributes to the reduction of the porosity. Nevertheless, the resulting structure is still a highly porous material. The latter could be also proved by the SEM micrographs obtained from the residues of the scaffolds that have been pyrolized at 850 °C in air. At the latter conditions only the inert inorganic part of the hybrid remains intact providing a very convenient way to study the morphology and the topology of the silica phase. Representative SEM micrographs are presented in Fig. 4c,d where a porous structure similar to that of the CHT can be observed.

It should be stressed that the potential use of the obtained porous structures described in the present paper is not limited to scaffolds for tissue engineering applications. The proposed strategy combined with the great versatility of the sol–gel method through the adjustment of the reaction parameters and the precursor ratio could allow the modification of the final porosity to meet the specific needs of various applications such as ultrafiltration, catalysis or pervaporation.

Table 2
Elastic modulus E′ obtained from stress–strain tests under tensile loading for dried and immersed in water samples.

Sample	Dried	Immersed
	E′ (MPa)	E′ (MPa)
CHT pure	1950	–
CHT–GEN (0.66 wt.%)	2320	–
CHT–GEN (3.2 wt.%)	3580	1.88
CHT–GEN (6.2 wt.%)	3750	2.12

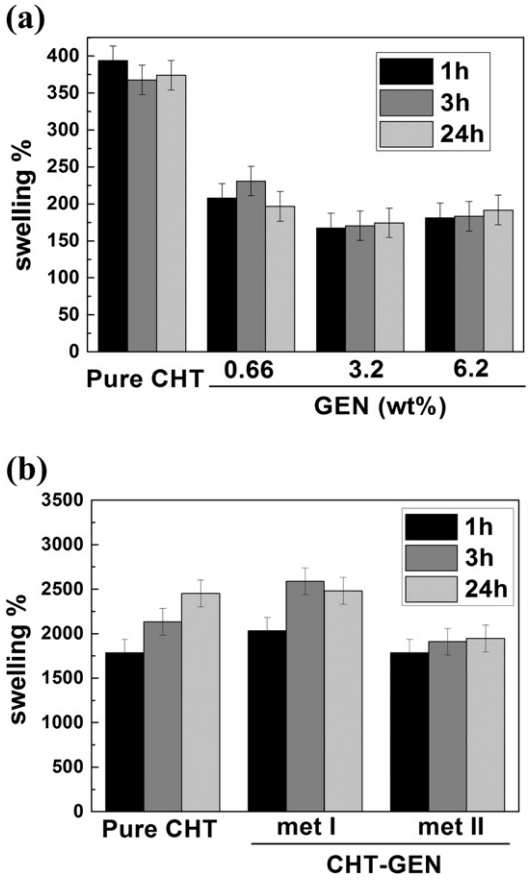

Fig. 3. Swelling behavior of CHT films cross-linked by method I with different GEN content (a) and comparison of CHT scaffolds cross-linked by the two methods (b).

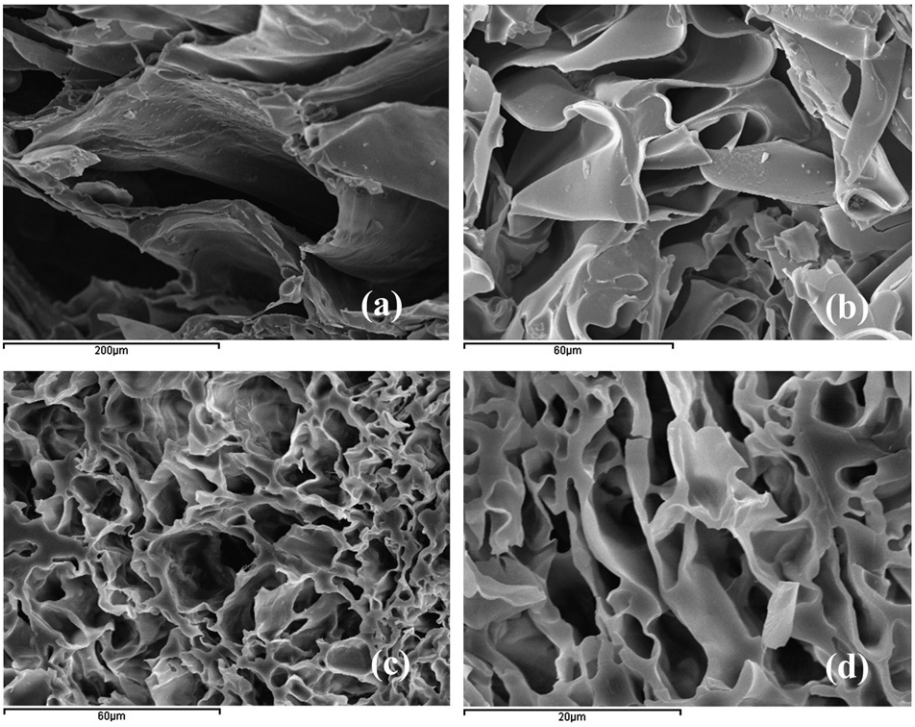

Fig. 4. SEM micrographs of CHTgenI + T/1G (a), CHTgenI + T/0.5G (b) the corresponding residue of the above materials after pyrolysis (c,d).

3.2.2. Thermogravimetric analysis

Thermogravimetric analysis was performed under nitrogen atmosphere from room temperature up to 800 °C. An initial weight loss at around 100 °C was observed, associated with the evaporation of water bound or trapped in the scaffolds. Chitosan exhibits a highly hydrophilic behavior [52] due to the hydroxyl and amino groups and the complete removal of water is difficult [53]. Furthermore, silica produced by sol–gel is also hydrophilic due to free silanol groups (Si–OH) that are always present in its surface. Previous studies have shown that the binding sites of silica prepared by sol–gel are already occupied by water molecules at a relative humidity level of 20% [54]. Fig. 5 shows TGA thermograms of CHT_{genI}, CHT_{genI} + T/0.5G and bulk TEOS/GPTMS 1:0.5 (coded as T/0.5G) starting at 150 °C, excluding, thus, the initial water loss due to evaporation, for the sake of comparison.

Pure chitosan and genipin cross-linked chitosan are characterized by the same thermal degradation profile (not shown here). The mass loss with a derivative peak located at 280 °C is assigned to the depolymerization of chitosan and generally varies with the molecular weight, the deacetylation degree [55] and the heating rate employed [56,57]. Briefly, the degradation of polysaccharide structure starts by a random scission of the glycosidic bonds followed by a further decomposition to form acetic and butyric acids and a series of lower fatty acids [58]. The results show that the method of chitosan cross-link does not affect thermal degradation behavior of chitosan.

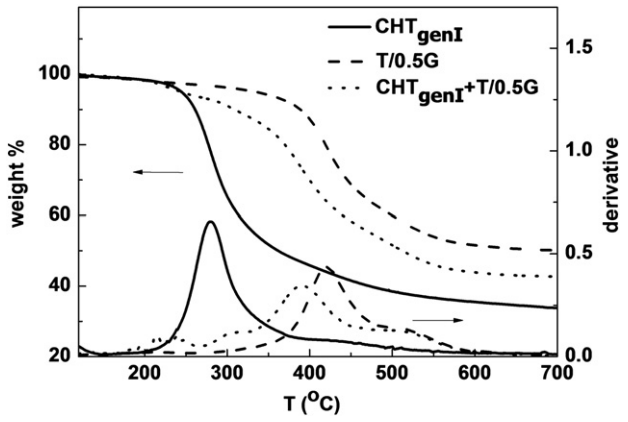

Fig. 5. TGA thermograms together with the corresponding derivative of CHTgenI, hybrid CHTgenI + T/0.5G and bulk T/0.5G.

On the contrary, the hybrid scaffolds incorporating GPTMS-TEOS present a three step degradation behavior appearing as three peaks in the derivative graphs (Fig. 5). The first peak at lower temperatures corresponds to the thermal degradation of chitosan while the other two at higher temperatures are associated with the thermal degradation of the introduced reinforcement component. The latter consists of an inorganic (silica from TEOS and GPTMS) and an organic (from GPTMS) part. The thermal degradation of the hybrids can be further studied by comparing their TGA thermograms and the corresponding derivative curves with those obtained on the pure components: CHT_{genI} and TEOS/GPTMS, produced in bulk which are also presented in Fig. 5. For the hybrids a more gradual weight loss is observed as well as an enhancement of thermal stability as compared to pure chitosan, indicated by the shift of 35 °C to higher temperatures of the derivative peak that corresponds to thermal degradation of chitosan.

Valuable information about the composition of the membranes could be extracted from the TGA experiments by evaluating the weight of the residue at the end of the heating scan. The values of the mass percentage of the residues are reported in Table 3 and refer to the dry mass of the samples after water removal. It is known that the thermal degradation of chitosan under nitrogen atmosphere is characterized by char formation [59]. A char residue of ~32% is obtained for the pure chitosan and CHT–GEN. As expected, higher residues are observed at the end of the heating scans for the scaffolds containing silica as the residue of the inert inorganic part is added to the chitosan char. Values between 41% and 51% are obtained for the scaffolds with varying TEOS/GPTMS ratio while the scaffolds with lower GPTMS content present higher silica content. Furthermore, the method of chitosan cross-linking does not affect the final silica content. The residues obtained from TGA at nitrogen atmosphere also differ from those after pyrolysis under oxidative

Table 3
Porosity, residue after pyrolysis and TGA, and E' calculated from the compressive stress–strain curves of the scaffolds immersed in water.

Sample	Code	TEOS-GPTMS weight after sol–gel	Porosity	Residue after pyrolysis	Residue TGA	E'
		%	%	%	%	(kPa)
CHT pure	CHT	–	95	–	32	10.4
CHT–GEN method I	CHT_{genI}	–	94	–	33	14.3
CHT–GEN method II	CHT_{genII}	–	95	–	33	46
CHT–GEN method I + TEOS/GPTMS 1:0.1	CHT_{genI} + T/0.1G	88	57	43	51	1732
CHT–GEN method I + TEOS/GPTMS 1:0.5	CHT_{genI} + T/0.5G	89	36	27	43	280
CHT–GEN method I + TEOS/GPTMS 1:1	CHT_{genI} + T/1G	74	64	26	41	106
CHT–GEN method II + TEOS/GPTMS 1:0.5	CHT_{genII} + T/0.5G	87	38	33	43	1590

conditions up to 850 °C as shown in Table 3. At the latter case no residue is observed for the pure and cross-linked chitosan. The above confirms the influence of the surrounding atmosphere on the thermal degradation behavior of chitosan reported in previous works [60]. The high weight loss at oxygen atmosphere is attributed to a very efficient chain scission with the formation of volatile degradation products due to oxidation followed by further decomposition of oxidized chitosan.

3.2.3. Differential scanning calorimetry

The thermal properties of the scaffolds were further studied by DSC from −80 °C up to 150 °C. The second heating scan was used to compare the thermal behavior of different samples after erasing the effect of any previous thermal history. No thermal transitions were observed for the pure chitosan samples. An endothermic peak due to water evaporation appeared in the first scan but was absent in the second one. Furthermore, no indication of a glass transition could be observed. There is a controversy in the literature regarding the glass transition of chitosan and many authors stress the difficulty of its study by DSC [55,61]. A glass transition temperature (T_g) has been ascribed at around 150 °C by combining different techniques [62].

Nevertheless, here we focus on a glass transition endothermic step appearing at temperatures below zero which appears only in scaffolds with TEOS/GPTMS and, thus, is attributed to the organic part formed by GPTMS. The DSC thermograms between −70 and −40 °C of the scaffolds are presented in Fig. 6 together with those corresponding to bulk TEOS/GPTMS 1:0.5 and TEOS/GPTMS 1:1 for the sake of comparison. A glass transition is observed in materials for GPTMS content ratio higher than 0.1 and the estimated T_g values are practically unaffected by GPTMS content and scaffold preparation method. The values of T_g as well as those of the heat capacity jump at each transition are listed in Table 4. Bulk TEOS/GPTMS samples present a glass transition around −45 to −50 ºC. The incorporation of GPTMS to the silica network disrupts its regularity due to the volume occupied by the organic side chains. The presence of the glass transition proves the cooperative conformational mobility of this organic/inorganic polymer network. Interestingly enough the glass transition is shifted to −60 ºC when

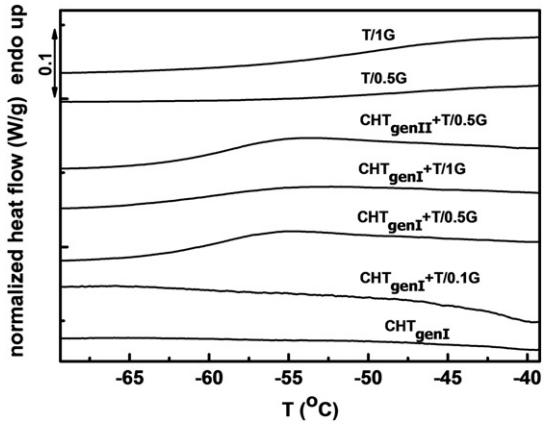

Fig. 6. DSC thermograms between −70 °C up to −40 °C during the second heating scan.

the TEOS/GPTMS is formed as a coating of the chitosan pore walls. This fact can be interpreted by assuming that the silica/organic structures formed in the coating layers are less ordered and, thus, with higher mobility than in the bulk. On the other hand, the heat capacity jump at the glass transition is larger in the coatings than in the bulk TEOS/GPTMS which means that a larger part of the network segments are involved in cooperative rearrangements. Interaction between organic groups of GPTMS and the polymeric walls can produce more disordered structures at the interface with the polymer.

3.2.4. Mechanical properties

Fig. 7 shows compressive stress–strain curves obtained by measurements performed in the samples immersed in water for the pure and cross-linked chitosan scaffolds as well as for those reinforced with silica. The elastic modulus has been calculated from the slope of the linear region of each curve and the results are reported in Fig. 7. A slight increase of E' can be observed by the cross-linking with GEN. As soon as the porosity is practically the same between CHT and CHT–GEN the strengthening effect is ascribed to cross-linking in agreement with the results presented in subsection 3.1.2. Furthermore, a significant increase on E' is observed for the scaffolds reinforced by silica which is more than one order of magnitude with the sample incorporating the lower quantity of GPTMS. The reduction of porosity (Table 1) also accounts for the increase of E' but the main contribution is due to the incorporation of a stiff silica material. It is worth noting the strong decrease of the modulus of the hybrid even for a small increase of GPTMS content (Table 1). This can be related to the increase of molecular mobility observed in DSC thermograms that makes coating layer more compliant. The latter observations imply that the mechanical properties of the chitosan scaffold could be controlled by changing the ratio of the silica precursors.

4. Conclusions

Silica reinforced membranes were prepared by the in situ synthesis of silica by sol–gel process inside the pores of chitosan scaffolds in acidic environment. The chitosan scaffolds were prepared by the freeze gelation technique and chitosan was cross-linked by genipin prior to silica introduction. The study regarding the optimum genipin concentration for the crosslinking procedure indicated that a GEN concentration of 3.2% is sufficient for rendering chitosan insoluble in acidic medium

Table 4
Results from DSC analysis about glass transition temperature (T_g) and heat capacity jump ΔC_p calculated from the second heating scan. ΔCp^* refers to the values normalized to GPTMS fraction of the sample.

Sample	T_g	ΔC_p	$\Delta C_p{}^*$
	°C	J/g.°C	J/g · °C
CHTgenI	–	–	–
CHTgenI + T/0.1G	–	–	–
CHTgenI + T/0.5G	60.1 ± 0.1	0.27 ± 0.02	1.72 ± 0.13
CHTgenI + T/1G	59.4 ± 0.3	0.21 ± 0.02	1.09 ± 0.10
CHTgenII + T/0.5G	59.9 ± 0.5	0.29 ± 0.02	1.52 ± 0.10
T/0.5G	44.5 ± 0.3	0.19 ± 0.02	0.33 ± 0.03
T/1G	50.1 ± 1.7	0.32 ± 0.02	0.43 ± 0.03

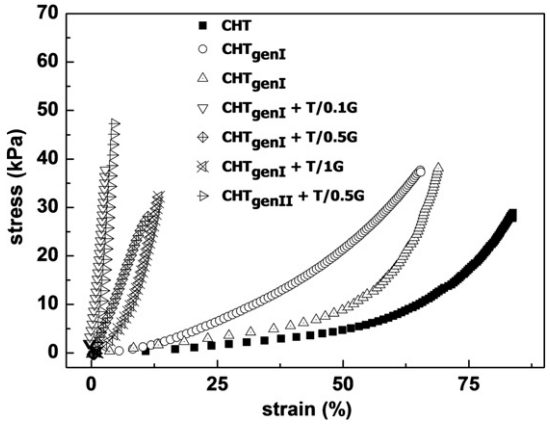

Fig. 7. Strain versus strain from compression tests on scaffolds immersed in water.

leaving at the same time adequate number of free amino groups to react with the silica precursors during the subsequent step of the preparation procedure. Two methods were examined for chitosan cross-linking by genipin either before or after scaffold preparation. The method in which the reaction with the cross-linking agent was performed by straight mixing at the chitosan solution prior to freeze gelation was favored as more efficient and simpler. The silica inorganic part was synthesized in situ using TEOS and GPTMS as silica precursors, the latter serving also as a coupling agent between the inorganic network and the hydrogel. The morphology studies revealed that the silica phase appears as a continuous phase covering the walls of the chitosan pores without affecting significantly the porosity of the scaffolds. By varying the TEOS/GPTMS ratio both, the porosity and the mechanical properties, as probed by compressive stress–strain tests, can be adjusted to meet specific needs. Finally, differential scanning calorimetry analysis allows the study of the glass transition of the separate GPTMS phase formed in the hybrids. More systematic DSC studies could shed some light towards understanding the admittedly complicated nature of GPTMS by evaluating its macroscopic properties in hybrid materials.

Acknowledgments

The research project is implemented within the framework of the Action "Supporting Postdoctoral Researchers" of the Operational Program "Education and Lifelong Learning" (Action's Beneficiary: General Secretariat for Research and Technology), and is co-financed by the European Social Fund (ESF) and the Greek State, Grant Number: NARGEL-PE5(2551). JFM thanks the Portuguese Foundation for Science and Technology (FCT) for financial support through the PTDC/FIS/115048/2009 project. JLGR acknowledges the support of the Ministerio de Economía y Competitividad, MINECO, through the MAT2013-46467-C4-1-R project.

References

[1] F. Shahidi, R. Abuzaytoun, Chitin, chitosan, and co-products: chemistry, production, applications, and health effects, Advances in Food and Nutrition Research, Academic Press, 2005. 93–135.
[2] M. Rinaudo, Chitin and chitosan: properties and applications, Prog. Polym. Sci. 31 (7) (2006) 603–632.
[3] M. Dash, F. Chiellini, R.M. Ottenbrite, E. Chiellini, Chitosan—a versatile semi-synthetic polymer in biomedical applications, Prog. Polym. Sci. 36 (8) (2011) 981–1014.
[4] T. Kean, M. Thanou, Biodegradation, biodistribution and toxicity of chitosan, Adv. Drug Deliv. Rev. 62 (1) (2010) 3–11.
[5] V.R. Sinha, A.K. Singla, S. Wadhawan, R. Kaushik, R. Kumria, K. Bansal, S. Dhawan, Chitosan microspheres as a potential carrier for drugs, Int. J. Pharm. 274 (1–2) (2004) 1–33.
[6] R. Jayakumar, M. Prabaharan, S.V. Nair, H. Tamura, Novel chitin and chitosan nanofibers in biomedical applications, Biotechnol. Adv. 28 (1) (2010) 142–150.
[7] S.V. Madihally, H.W.T. Matthew, Porous chitosan scaffolds for tissue engineering, Biomaterials 20 (12) (1999) 1133–1142.
[8] S. Despond, E. Espuche, N. Cartier, A. Domard, Hydration mechanism of polysaccharides: a comparative study, J. Polym. Sci., Part B: Polym. Phys. 43 (1) (2005) 48–58.
[9] R.A.A. Muzzarelli, Chitins and chitosans for the repair of wounded skin, nerve, cartilage and bone, Carbohydr. Polym. 76 (2) (2009) 167–182.
[10] I.Y. Kim, S.J. Seo, H.S. Moon, M.K. Yoo, I.Y. Park, B.C. Kim, C.S. Cho, Chitosan and its derivatives for tissue engineering applications, Biotechnol. Adv. 26 (1) (2008) 1–21.
[11] X. Liu, L. Ma, Z. Mao, C. Gao, Chitosan-based biomaterials for tissue repair and regeneration, in: R. Jayakumar, M. Prabaharan, R.A.A. Muzzarelli (Eds.), Chitosan for Biomaterials II, Springer, Berlin Heidelberg, 2011, pp. 81–127.
[12] R. Jayakumar, M. Prabaharan, P.T. Sudheesh Kumar, S.V. Nair, H. Tamura, Biomaterials based on chitin and chitosan in wound dressing applications, Biotechnol. Adv. 29 (3) (2011) 322–337.
[13] I.-Y. Kim, S.-J. Seo, H.-S. Moon, M.-K. Yoo, I.-Y. Park, B.-C. Kim, C.-S. Cho, Chitosan and its derivatives for tissue engineering applications, Biotechnol. Adv. 26 (1) (2008) 1–21.
[14] N.M. Alves, J.F. Mano, Chitosan derivatives obtained by chemical modifications for biomedical and environmental applications, Int. J. Biol. Macromol. 43 (5) (2008) 401–414.
[15] J. Berger, M. Reist, J.M. Mayer, O. Felt, N.A. Peppas, R. Gurny, Structure and interactions in covalently and ionically crosslinked chitosan hydrogels for biomedical applications, Eur. J. Pharm. Biopharm. 57 (1) (2004) 19–34.
[16] X.Z. Shu, K.J. Zhu, A novel approach to prepare tripolyphosphate/chitosan complex beads for controlled release drug delivery, Int. J. Pharm. 201 (1) (2000) 51–58.
[17] R.A.A. Muzzarelli, Genipin-crosslinked chitosan hydrogels as biomedical and pharmaceutical aids, Carbohydr. Polym. 77 (1) (2009) 1–9.
[18] J. Jin, M. Song, D.J. Hourston, Novel chitosan-based films cross-linked by genipin with improved physical properties, Biomacromolecules 5 (1) (2003) 162–168.
[19] F.L. Mi, Y.C. Tan, H.F. Liang, H.W. Sung, In vivo biocompatibility and degradability of a novel injectable-chitosan-based implant, Biomaterials 23 (1) (2002) 181–191.
[20] Y. Huang, S. Onyeri, M. Siewe, A. Moshfeghian, S.V. Madihally, In vitro characterization of chitosan-gelatin scaffolds for tissue engineering, Biomaterials 26 (36) (2005) 7616–7627.
[21] Y.T. Jia, J. Gong, X.H. Gu, H.Y. Kim, J. Dong, X.Y. Shen, Fabrication and characterization of poly (vinyl alcohol)/chitosan blend nanofibers produced by electrospinning method, Carbohydr. Polym. 67 (3) (2007) 403–409.
[22] M.N.V. Ravi Kumar, U. Bakowsky, C.M. Lehr, Preparation and characterization of cationic PLGA nanospheres as DNA carriers, Biomaterials 25 (10) (2004) 1771–1777.
[23] C. Gu, W. Shi, M. Lang, Enhanced mechanical property of chitosan via blending with functional poly(ε-caprolactone), J. Polym. Sci., Part B: Polym. Phys. 51 (8) (2013) 659–667.
[24] S.C. Neves, L.S. Moreira Teixeira, L. Moroni, R.L. Reis, C.A. Van Blitterswijk, N.M. Alves, M. Karperien, J.F. Mano, Chitosan/Poly(ε-caprolactone) blend scaffolds for cartilage repair, Biomaterials 32 (4) (2011) 1068–1079.
[25] I. Yamaguchi, K. Tokuchi, H. Fukuzaki, Y. Koyama, K. Takakuda, H. Monma, J. Tanaka, Preparation and microstructure analysis of chitosan/hydroxyapatite nanocomposites, J. Biomed. Mater. Res. 55 (1) (2001) 20–27.
[26] X. Wang, Y. Du, J. Luo, B. Lin, J.F. Kennedy, Chitosan/organic rectorite nanocomposite films: Structure, characteristic and drug delivery behaviour, Carbohydr. Polym. 69 (1) (2007) 41–49.
[27] S.F. Wang, L. Shen, W.D. Zhang, Y.J. Tong, Preparation and mechanical properties of chitosan/carbon nanotubes composites, Biomacromolecules 6 (6) (2005) 3067–3072.
[28] E.J. Lee, D.S. Shin, H.E. Kim, H.W. Kim, Y.H. Koh, J.H. Jang, Membrane of hybrid chitosan–silica xerogel for guided bone regeneration, Biomaterials 30 (5) (2009) 743–750.
[29] W.J.E.M. Habraken, J.G.C. Wolke, J.A. Jansen, Ceramic composites as matrices and scaffolds for drug delivery in tissue engineering, Adv. Drug Deliv. Rev. 59 (4–5) (2007) 234–248.
[30] S.G. Caridade, E.G. Merino, N.M. Alves, VdZ Bermudez, A.R. Boccaccini, J.F. Mano, Chitosan membranes containing micro or nano-size bioactive glass particles: evolution of biomineralization followed by in situ dynamic mechanical analysis, J. Mech. Behav. Biomed. 20 (2013) 173–183.
[31] G.M. Luz, J.F. Mano, Chitosan/bioactive glass nanoparticles composites for biomedical applications, Biomed. Mater. 7 (5) (2012) 054104.
[32] S. Spirk, G. Findenig, A. Doliska, V.E. Reichel, N.L. Swanson, R. Kargl, V. Ribitsch, K. Stana-Kleinschek, Chitosan–silane sol–gel hybrid thin films with controllable layer thickness and morphology, Carbohydr. Polym. 93 (1) (2013) 285–290.
[33] Y. Shirosaki, K. Tsuru, S. Hayakawa, A. Osaka, M.A. Lopes, J.D. Santos, M.A. Costa, M.H. Fernandes, Physical, chemical and in vitro biological profile of chitosan hybrid membrane as a function of organosiloxane concentration, Acta Biomater. 5 (1) (2009) 346–355.
[34] C.-Y. Hsieh, S.-P. Tsai, D.-M. Wang, Y.-N. Chang, H.-J. Hsieh, Preparation of γ-PGA/chitosan composite tissue engineering matrices, Biomaterials 26 (28) (2005) 5617–5623.
[35] E.M. Valliant, J.R. Jones, Softening bioactive glass for bone regeneration: sol–gel hybrid materials, Soft Matter 7 (11) (2011) 5083–5095.
[36] S.S. Silva, J.M. Oliveira, J.F. Mano, R.L. Reis, Physicochemical Characterization Of Novel Chitosan–Soy Protein/TEOS Porous Hybrids For Tissue Engineering Applications, 2006. (514-5161000-1004).
[37] Y. Shirosaki, T. Okayama, K. Tsuru, S. Hayakawa, A. Osaka, Synthesis and cytocompatibility of porous chitosan-silicate hybrids for tissue engineering scaffold application, Chem. Eng. J. 137 (1) (2008) 122–128.
[38] M.H. Ho, P.Y. Kuo, H.J. Hsieh, T.Y. Hsien, L.T. Hou, J.Y. Lai, D.M. Wang, Preparation of porous scaffolds by using freeze-extraction and freeze-gelation methods, Biomaterials 25 (1) (2004) 129–138.
[39] C.J. Brinker, G.W. Scherer, Sol–gel science, The Physics and Chemistry of Sol–gel Processing, Academic Press Inc, Boston, 1990.

[40] C.E. Plazas Bonilla, J.A. Gómez-Tejedor, J.E. Perilla, J.L. Gómez Ribelles, Silica phase formed by sol–gel reaction in the nano- and micro-pores of a polymer hydrogel, J. Non-Cryst. Solids (2013) 37912–37920.
[41] B. Demirdögen, C.E. Plazas Bonilla, S. Trujillo, J.E. Perilla, A.E. Elcin, Y.M. Elcin, J.L. Gómez Ribelles, Silica coating of the pore walls of a microporous polycaprolactone membrane to be used in bone tissue engineering, J. Biomed. Mater. Res. A (2013), http://dx.doi.org/10.1002/jbm.a.34999.
[42] C.-Y. Hsieh, S.-P. Tsai, M.-H. Ho, D.-M. Wang, C.-E. Liu, C.-H. Hsieh, H.-C. Tseng, H.-J. Hsieh, Analysis of freeze-gelation and cross-linking processes for preparing porous chitosan scaffolds, Carbohydr. Polym. 67 (1) (2007) 124–132.
[43] E. Curotto, F. Aros, Quantitative determination of chitosan and the percentage of free amino groups, Anal. Biochem. 211 (2) (1993) 240–241.
[44] M.F. Butler, Y.F. Ng, P.D.A. Pudney, Mechanism and kinetics of the crosslinking reaction between biopolymers containing primary amine groups and genipin, J. Polym. Sci. A Polym. Chem. 41 (24) (2003) 3941–3953.
[45] F. Croisier, C. Jérôme, Chitosan-based biomaterials for tissue engineering, Eur. Polym. J. 49 (4) (2013) 780–792.
[46] A. Abarrategi, Y. Lópiz-Morales, V. Ramos, A. Civantos, L. López-Dufn, F. Marco, J.L. López-Lacomba, Chitosan scaffolds for osteochondral tissue regeneration, J. Biomed. Mater. Res. A 95 (4) (2010) 1132–1141.
[47] R. Seda Ti li, A. Karakeçili, M. Gumusderelioglu, In vitro characterization of chitosan scaffolds: influence of composition and deacetylation degree, J. Mater. Sci. Mater. Med. 18 (9) (2007) 1665–1674.
[48] G. Wang, Q. Ao, K. Gong, A. Wang, L. Zheng, Y. Gong, X. Zhang, The effect of topology of chitosan biomaterials on the differentiation and proliferation of neural stem cells, Acta Biomater. 6 (9) (2010) 3630–3639.
[49] C. Pandis, S. Trujillo, M. Roganowicz, J.L. Gómez Ribelles, Hybrid polycaprolactone/silica porous membranes produced by sol–gel, Macromol. Symp. (2014) (in press).
[50] L.S. Connell, F. Romer, M. Suarez, E.M. Valliant, Z. Zhang, P.D. Lee, M.E. Smith, J.V. Hanna, J.R. Jones, Chemical characterisation and fabrication of chitosan–silica hybrid scaffolds with 3-glycidoxypropyl trimethoxysilane, J. Mater. Chem. B 2 (6) (2014) 668–680.
[51] L. Gabrielli, L. Russo, A. Poveda, J.R. Jones, F. Nicotra, J. Jiménez-Barbero, L. Cipolla, Epoxide opening versus silica condensation during sol–gel hybrid biomaterial synthesis, Chem. Eur. J. 19 (24) (2013) 7856–7864.
[52] S. Ludwiczak, M. Mucha, Modeling of water sorption isotherms of chitosan blends, Carbohydr. Polym. 79 (1) (2010) 34–39.
[53] M.T. Viciosa, M. Dionísio, J.F. Mano, Dielectric characterization of neutralized and nonneutralized chitosan upon drying, Biopolymers 81 (3) (2006) 149–159.
[54] C. Pandis, A. Spanoudaki, A. Kyritsis, P. Pissis, J.C.R. Hernández, J.L. Gõmez Ribelles, Pradas M. Monleõn, Water sorption characteristics of poly(2-hydroxyethyl acrylate)/silica nanocomposite hydrogels, J. Polym. Sci., Part B: Polym. Phys. 49 (9) (2011) 657–668.
[55] F.S. Kittur, K.V. Harish Prashanth, K. Udaya Sankar, R.N. Tharanathan, Characterization of chitin, chitosan and their carboxymethyl derivatives by differential scanning calorimetry, Carbohydr. Polym. 49 (2) (2002) 185–193.
[56] V. Georgieva, D. Zvezdova, L. Vlaev, Non-isothermal kinetics of thermal degradation of chitosan, Chem. Cent. J. 6 (1) (2012) 1–10.
[57] D. de Britto, S.P. Campana-Filho, Kinetics of the thermal degradation of chitosan, Thermochim. Acta 465 (1–2) (2007) 73–82.
[58] F.A. López, A.L.R. Mercê, F.J. Alguacil, A. López-Delgado, A kinetic study on the thermal behaviour of chitosan, J. Therm. Anal. Calorim. 91 (2) (2008) 633–639.
[59] T. Wanjun, W. Cunxin, C. Donghua, Kinetic studies on the pyrolysis of chitin and chitosan, Polym. Degrad. Stab. 87 (3) (2005) 389–394.
[60] J. Zawadzki, H. Kaczmarek, Thermal treatment of chitosan in various conditions, Carbohydr. Polym. 80 (2) (2010) 394–400.
[61] K. Sakurai, T. Maegawa, T. Takahashi, Glass transition temperature of chitosan and miscibility of chitosan/poly(N-vinyl pyrrolidone) blends, Polymer 41 (19) (2000) 7051–7056.
[62] Y. Dong, Y. Ruan, H. Wang, Y. Zhao, D. Bi, Studies on glass transition temperature of chitosan with four techniques, J. Appl. Polym. Sci. 93 (4) (2004) 1553–1558.

Christos Pandis was born in Athens, Greece in 1978. He graduated from the University of Athens in 2003 with a Diploma in Physics. He obtained his M.Sc in Microsystems and Nanodevices in 2005 and his PhD in Materials Science–Physics in 2010, both at the National Technical University of Athens. He is currently a post-doctoral researcher at the Centro de Biomateriales e Ingeniería Tisular, Universitat Politècnica de València. He has published 19 journal papers and his research focuses on hybrid biomaterials and the study of structure–property relationship of polymers and polymer nanocomposites.

Sara Madeira was born in Braga, Portugal in 1990. She obtained her Master's Degree in Biomedical Engineering—Biomaterials, Rehabilitation and Biomechanical at the University of Minho in 2013. During her thesis she made a six month scientific visit at the Centro de Biomateriales e Ingenieria Tissular, Universitat Politécnica de València.

Joana Matos was born in Paris, France in 1990 and she moved to Portugal in 1999 to Viana do Castelo. She is a Biomedical Engineer, specialized in the area of Biomaterials, Biomechanics and Rehabilitation, graduated at the University of Minho, Braga (Portugal) in 2013. During her degree she made a six month scientific visit at the Centro de Biomateriales e Ingenieria Tissular, Universitat Politécnica de València. The title of her dissertation was 'Development of a 3D multibody system of the human lumbar spine'.

Apostolos Kyritsis was born in Berlin, Germany in 1966. He received the Diploma in Physics in 1988 and the Ph.D. Degree in Materials Science–Physics in 1995 both by the University of Athens, Greece. He is an Assistant Professor at the Physics Department, National Technical University of Athens—NTUA, Greece. He has published more than 60 scientific papers, more than 20 papers in conference proceedings and 3 book chapters. His scientific interests include dielectric, calorimetric and vapor sorption studies in ionic crystals, ceramics, polymers and complex polymeric systems and structure–property relationships in polymers, biopolymers and nanocomposites

João F. Mano received his PhD in Chemistry in 1996 from the Technical University of Lisbon. Currently he is an Associate Professor with Habilitation at the Polymer Engineering Department, School of Engineering, University of Minho, Portugal, and he is a vice-director of the 3B's research group, Biomaterials, Biodegradables and Biomimetics, which is a member of the ICVS/3B's Associate Laboratory. João F. Mano is an author of 480+ works listed in the ISI–WebOfScience (390+ scientific papers, 7100+ citations, 26 book chapters and three patents. João F. Mano co-edited three special issues in international journals and three books. He presented 33 invited lectures in international meetings.

José Luis Gómez Ribelles is a Professor at the Universidad Politécnica de Valencia, Spain, UPV, since 1993. He is the director of the Centre for Biomaterials and Tissue Engineering of the UPV since 2008, member of the Spanish National Network for Cell Therapy and researcher at the Networking Research Center on Bioengineering, Biomaterials and Nanomedicine (CIBER-BBN). Prof. J.L. Gómez Ribelles is an author of more than 200 papers in indexed scientific journals that have been cited more than 2000 times, two books, 13 invited lectures and around 200 communications to scientific conferences.